Molecular Cell, Volume *57*

Supplemental Information

The Strength and Cooperativity of KIT Ectodomain Contacts Determine Normal Ligand-Dependent Stimulation or Oncogenic Activation in Cancer

Andrey V. Reshetnyak, Yarden Opatowsky, Titus J. Boggon,
Ewa Folta-Stogniew, Francisco Tome, Irit Lax, and Joseph Schlessinger

Figure S1

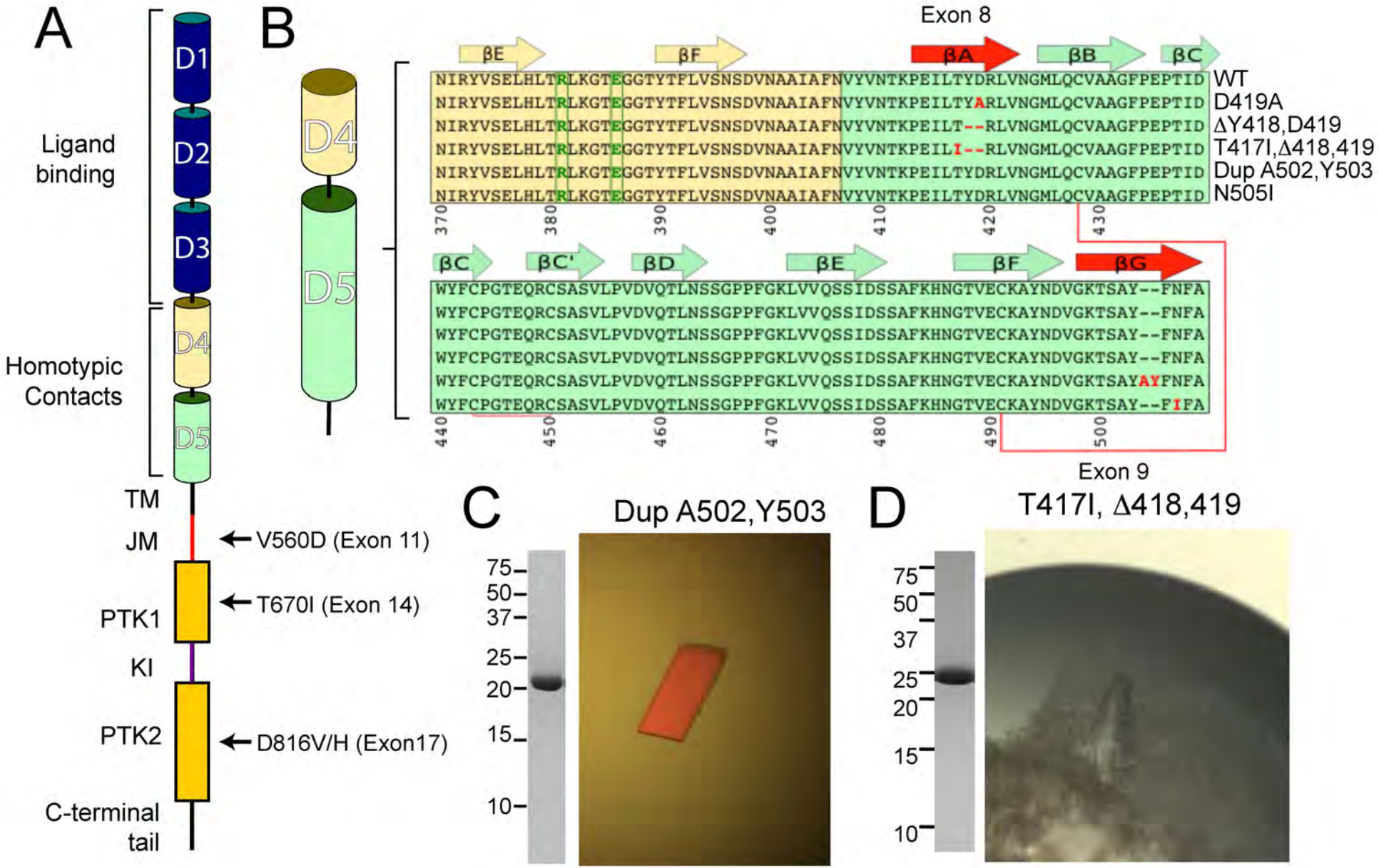
A
Ligand binding
D1
D2
D3
Homotypic Contacts
D4
D5
TM
JM
V560D (Exon 11)
PTK1
T670I (Exon 14)
KI
PTK2
D816V/H (Exon17)
C-terminal tail
B
D4
D5
Exon 8
βE
βF
βA
βB
βC
NIRYVSELHLTRLKGTEGGTYTFLVSNSDVNAAIAFNVYVNTKPEILTYDRLVNGMLQCVAAGFPEPTID WT
NIRYVSELHLTRLKGTEGGTYTFLVSNSDVNAAIAFNVYVNTKPEILTYARLVNGMLQCVAAGFPEPTID D419A
NIRYVSELHLTRLKGTEGGTYTFLVSNSDVNAAIAFNVYVNTKPEILT--RLVNGMLQCVAAGFPEPTID ΔY418,D419
NIRYVSELHLTRLKGTEGGTYTFLVSNSDVNAAIAFNVYVNTKPEIL I--RLVNGMLQCVAAGFPEPTID T417I,Δ418,419
NIRYVSELHLTRLKGTEGGTYTFLVSNSDVNAAIAFNVYVNTKPEILTYDRLVNGMLQCVAAGFPEPTID Dup A502,Y503
NIRYVSELHLTRLKGTEGGTYTFLVSNSDVNAAIAFNVYVNTKPEILTYDRLVNGMLQCVAAGFPEPTID N505I
370 380 390 400 410 420 430
βC βC' βD βE βF βG
WYFCPGTEQRCSASVLPVDVQTLNSSGPPFGKLVVQSSIDSSAFKHNGTVECKAYNDVGKTSAY--FNFA
WYFCPGTEQRCSASVLPVDVQTLNSSGPPFGKLVVQSSIDSSAFKHNGTVECKAYNDVGKTSAY--FNFA
WYFCPGTEQRCSASVLPVDVQTLNSSGPPFGKLVVQSSIDSSAFKHNGTVECKAYNDVGKTSAY--FNFA
WYFCPGTEQRCSASVLPVDVQTLNSSGPPFGKLVVQSSIDSSAFKHNGTVECKAYNDVGKTSAY--FNFA
WYFCPGTEQRCSASVLPVDVQTLNSSGPPFGKLVVQSSIDSSAFKHNGTVECKAYNDVGKTSAYAYFNFA
WYFCPGTEQRCSASVLPVDVQTLNSSGPPFGKLVVQSSIDSSAFKHNGTVECKAYNDVGKTSAY--FIFA
440 450 460 470 480 490 500
C
Dup A502,Y503
75 50 37 25 20 15 10
D
Exon 9
T417I, Δ418,419
75 50 37 25 20 15 10

Figure S2

A

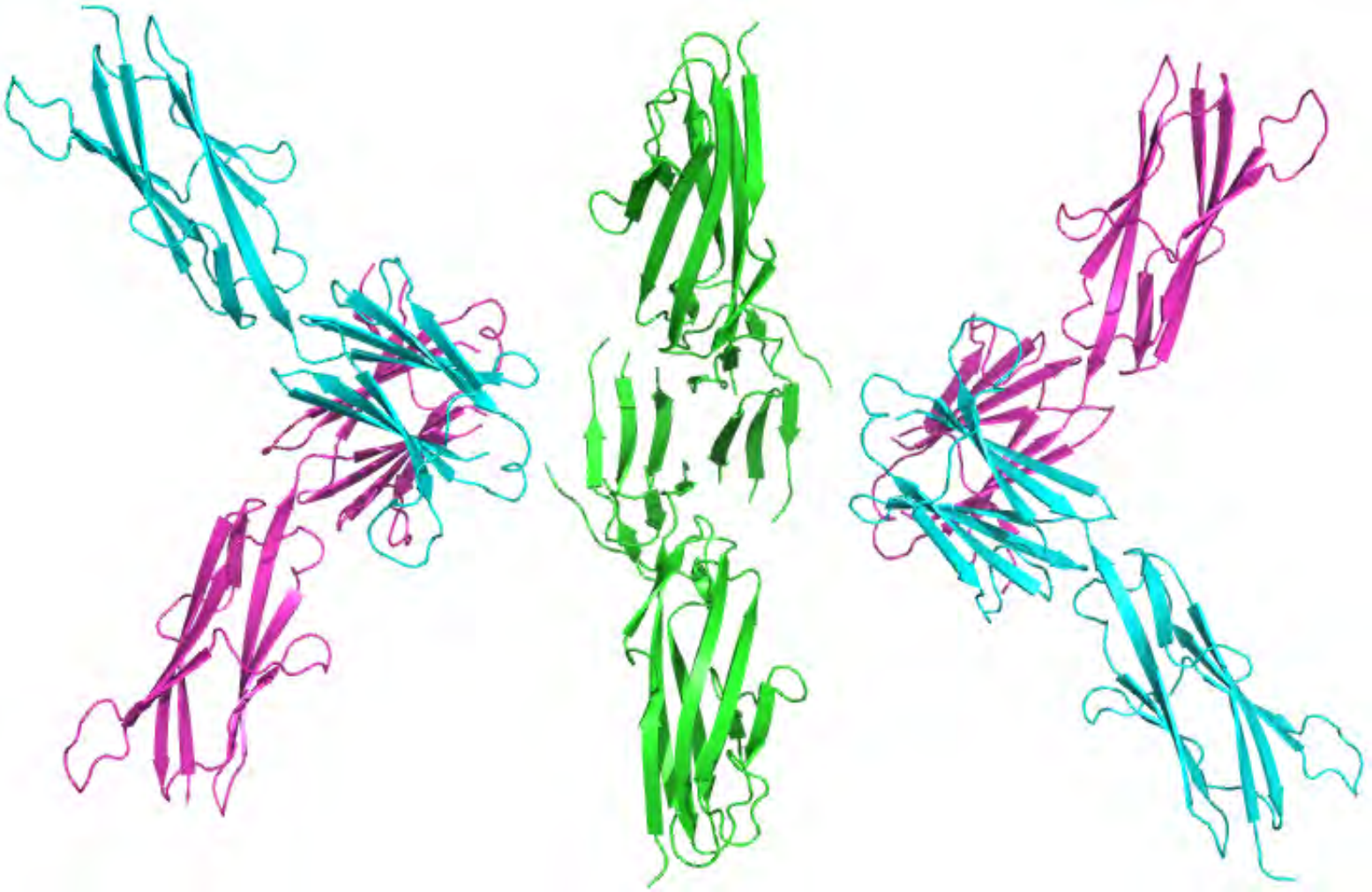

B

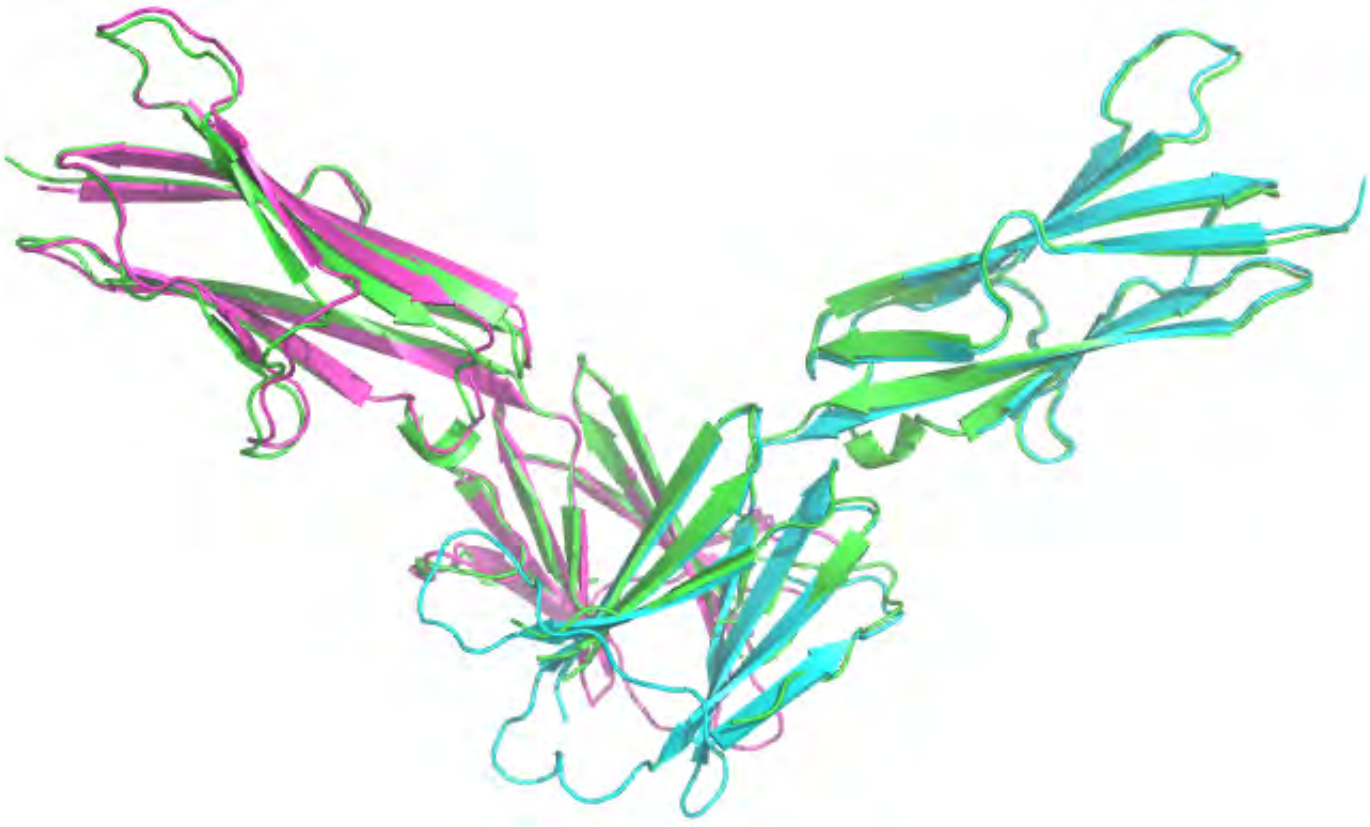

Figure S3

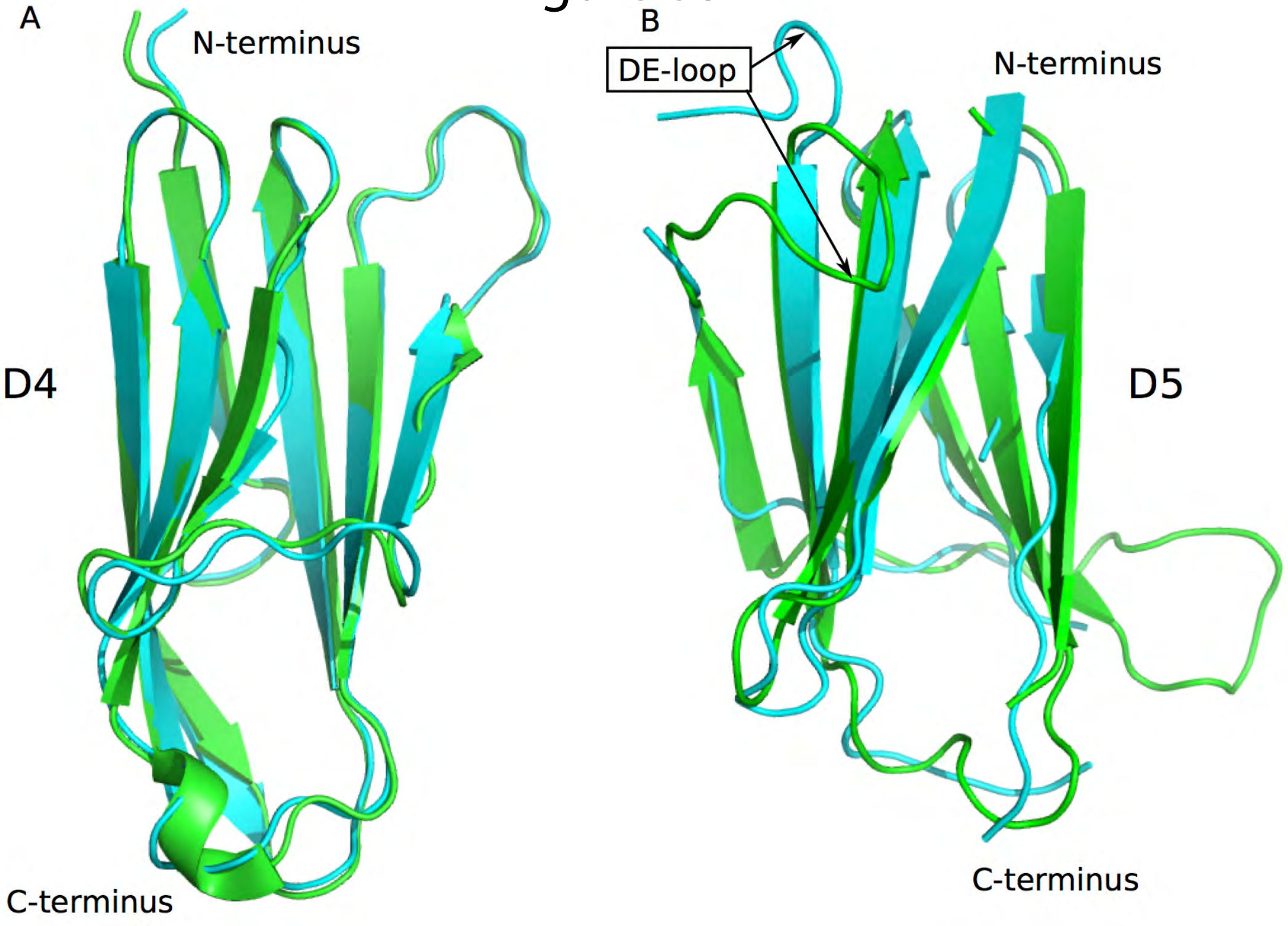

Figure S4

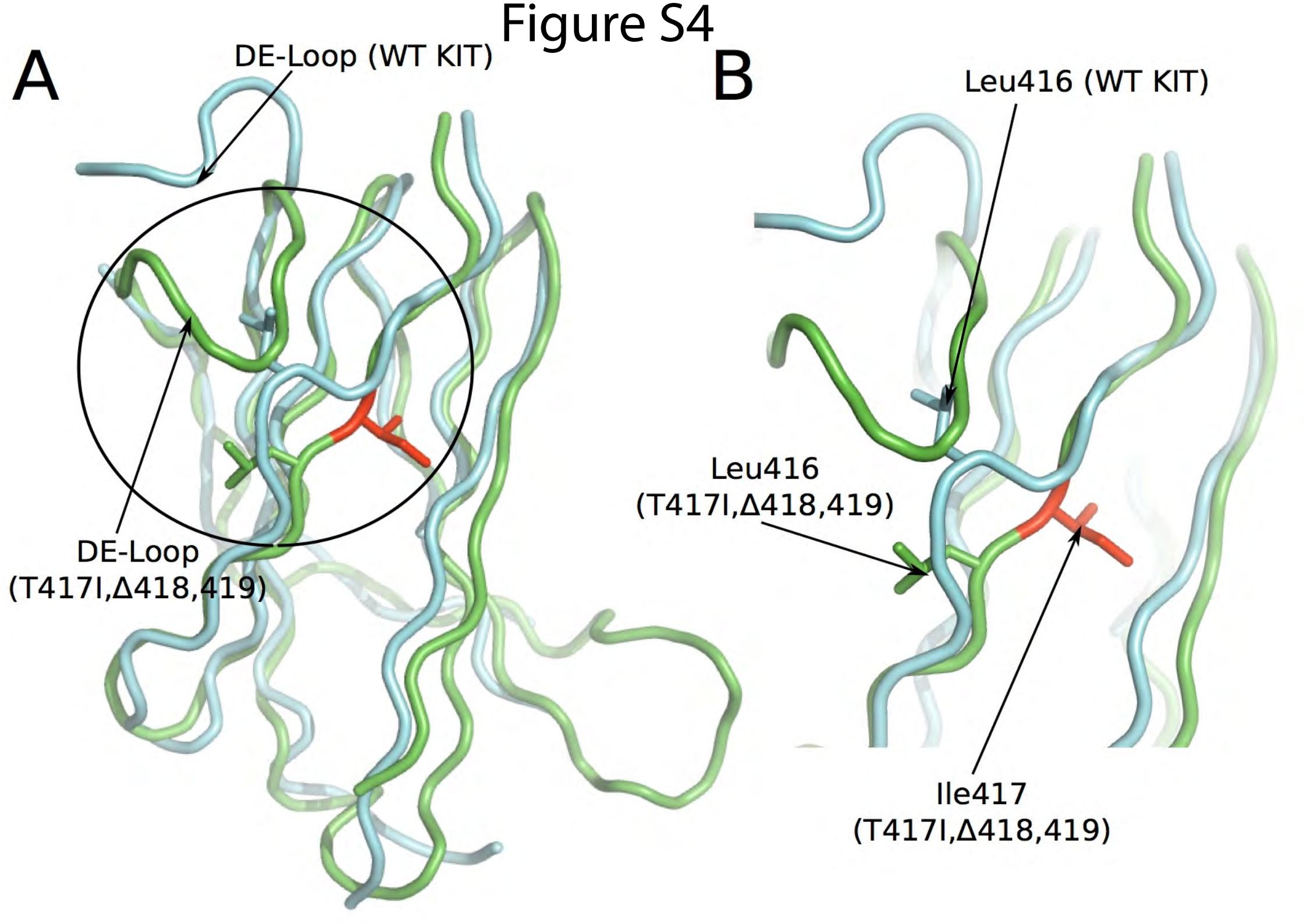
A
DE-Loop (WT KIT)
DE-Loop
(T417I,Δ418,419)
B
Leu416 (WT KIT)
Leu416
(T417I,Δ418,419)
Ile417
(T417I,Δ418,419)

Figure S5

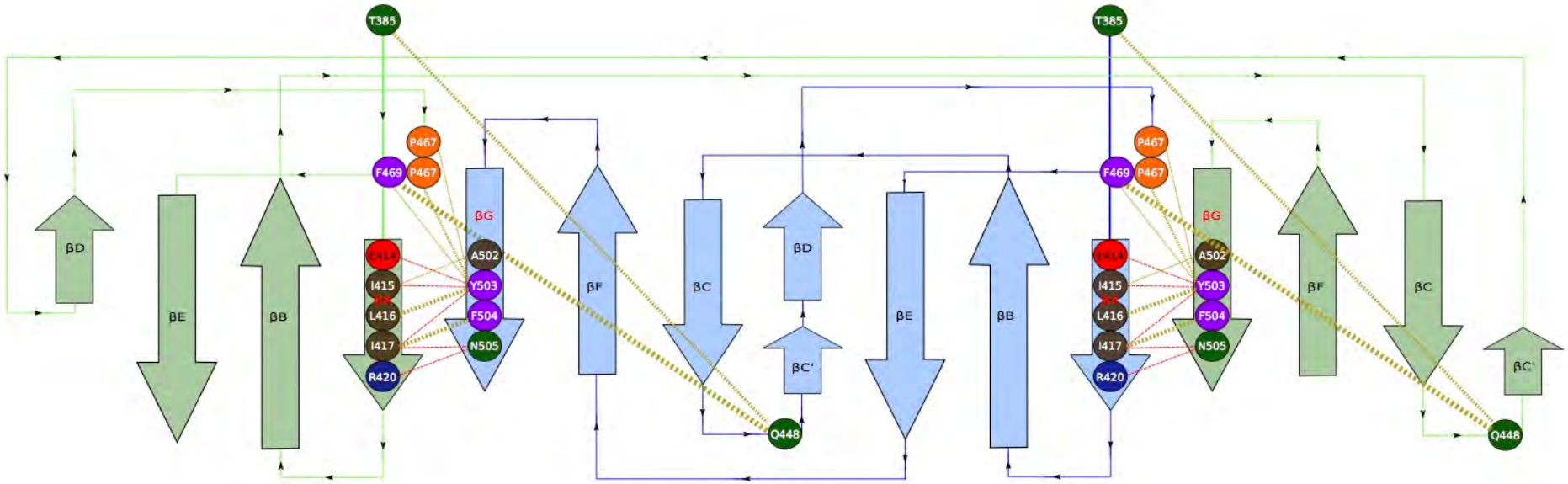
T385
P467
F469
P467
βG
E414
I415
L416
I417
R420
A502
Y503
F504
N505
βD
βE
βB
βF
βC
βC'
Q448
T385
P467
F469
P467
βG
E414
I415
L416
I417
R420
A502
Y503
F504
N505
βD
βE
βB
βF
βC
βC'
Q448

Figure S6

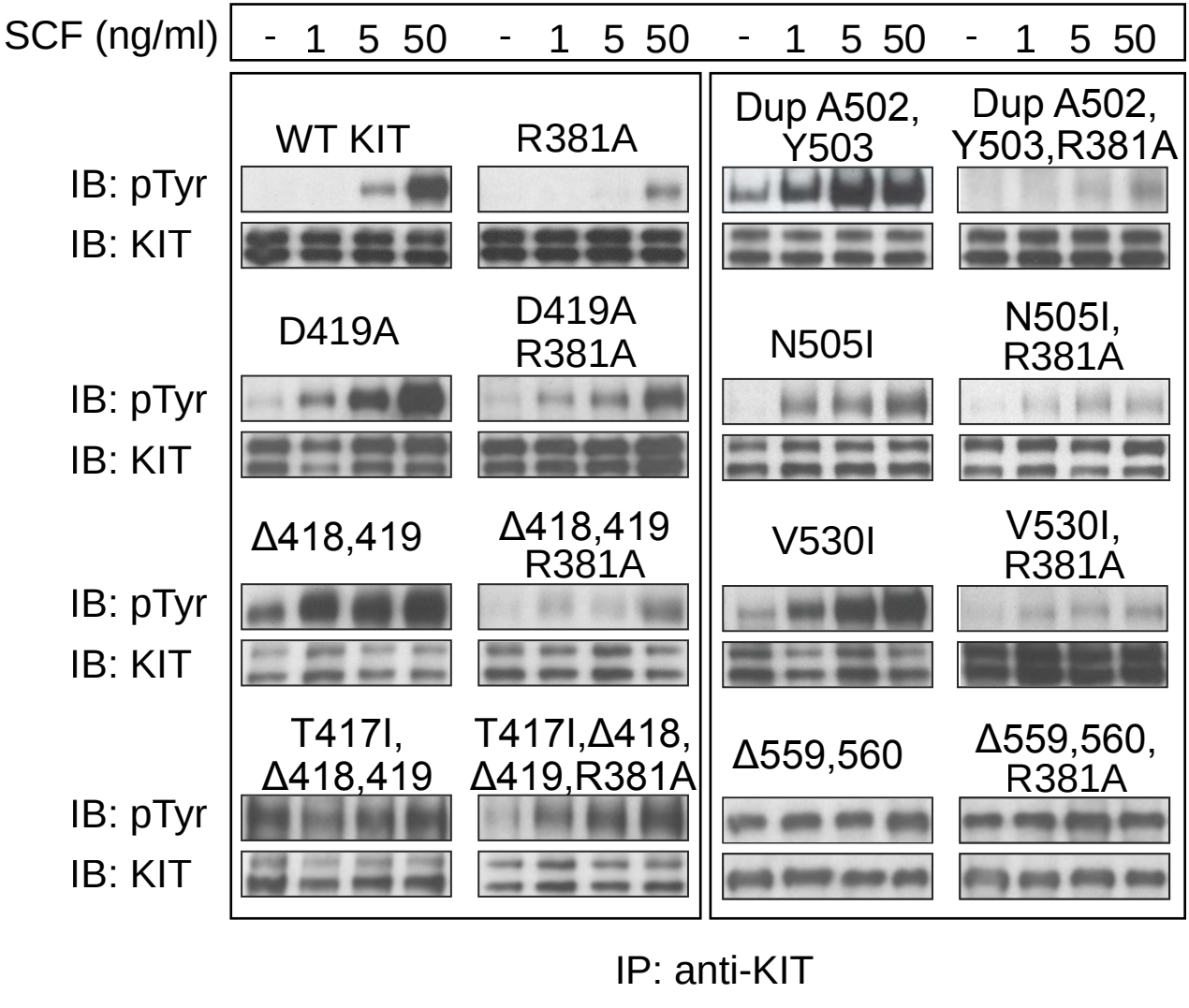
SCF (ng/ml)
- 1 5 50 - 1 5 50 - 1 5 50 - 1 5 50
WT KIT
R381A
Dup A502, Y503
Dup A502, Y503,R381A
D419A
D419A R381A
N505I
N505I, R381A
Δ418,419
Δ418,419 R381A
V530I
V530I, R381A
T417I, Δ418,419
T417I,Δ418, Δ419,R381A
Δ559,560
Δ559,560, R381A
IB: pTyr
IB: KIT
IB: pTyr
IB: KIT
IB: pTyr
IB: KIT
IB: pTyr
IB: KIT
IP: anti-KIT

Figure S7

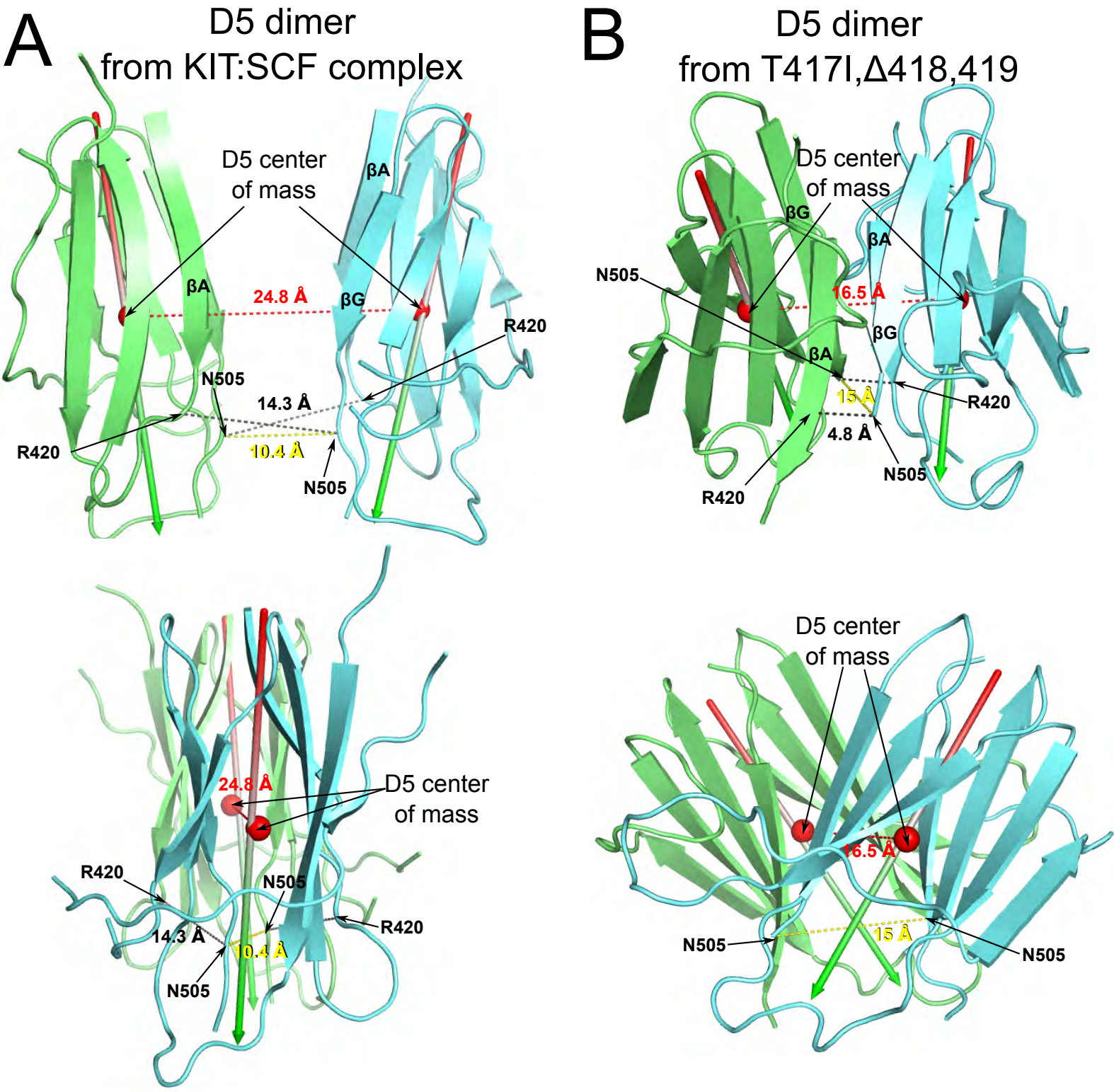
A
D5 dimer
from KIT:SCF complex
D5 center
of mass
βA
βG
24.8 Å
R420
N505
14.3 Å
10.4 Å
B
D5 dimer
from T417I,Δ418,419
16.5 Å
15 Å
4.8 Å

SUPPLEMENTARY MATERIAL

Figure Legends:

Figure S1. Related to Figure 1, Overview of KIT oncogenic mutants.
(A) Schematic representation of full length KIT receptor. D1 – D5 are Ig-like domains. D1-D3 are represented as cylinders colored in blue, D4 in yellow and D5 in green. TM is transmembrane (black), JM - juxtamembrane (red), PTK - protein tyrosine kinase (yellow), KI - kinase insert (purple) domains.
(B) Sequence alignment of oncogenic mutants in KIT D5. D4 is highlighted with yellow and D5 with green. β strands of Ig-like domains are shown with arrows on top of sequence alignment. Oncogenic hot spots are highlighted in red. Cysteine bridges are shown with red lines. (C) and (D) SDS PAGE analysis of purified protein samples used for crystallization (left panel) and pictures of protein crystals (right panel) of Dup502,503 D4D5 mutant (C) and T417, Δ418,419 D4D5 mutant (D).

Figure S2. Related to Figure 1, KIT T417I,Δ418,419 D4D5 dimer assembly in the asymmetric unit.
A. Cartoon representation of T417I,Δ418,419 D4D5 structure, molecules from two neighboring ASU are represented. There are 3 molecules in each ASU and different chains are colored with cyan, magenta and green. Molecules, which are colored in cyan and magenta, are making dimers in the same ASU. Two green molecules belong to the different ASU and make the same dimeric assembly as cyan and magenta D4D5s. As D5 colored in green has higher B factor the majority of amino acids of the dimer interface could not be built.
B. Alignment of symmetry mate dimers. Two dimeric assemblies from A are aligned to each other. A superposition of Cα atoms gave RMSD of 0.7 Å over 274 carbon alphas.

Figure S3. Related to Figure 1, Structural alignment of individual D4 and D5 domains of KIT ectodomain and T417I, Δ418,419 D4D5 mutant.
Cartoon representation of individual D4 (A) and D5 (B) domains. D4 and D5 from KIT

ectodomain (PDB code: 2EC8, Yuzawa et al., 2007) are shown in cyan. D4 and D5 from T417I, Δ418,419 KIT D4D5 structure are shown in green. Difference in folding of the DE-loop is marked by arrows.

Figure S4. Related to Figure 1, Clashing of Leu416 from WT KIT with DE-loop from T417I, Δ418,419 mutant.

Ribbon representation of D5 domains. D5 domain from KIT ectodomain (PDB code: 2EC8, Yuzawa et al., 2007) is shown in cyan and from T417I, Δ418,419 mutant in green. Ile417 (oncogenic mutation) in T417I, Δ418,419 mutant is highlighted with red. Clash between WT KIT and T417I, Δ418,419 mutant is shown by circle. (B) close up view.

Figure S5. Related to Figure 4, 2D representation of D5:D5 interface of T417I, Δ418,419 mutant.

Schematic representation of D5:D5 dimer interface. One protomer is colored in cyan and another protomer is in green. Beta strands are represented with arrows. Hydrogen bonds are shown with red dashes and hydrophobic interactions with golden dashes. Residues involved in mediating dimer interface formation are shown with circles and numbered according to amino acid sequence of WT KIT. Interface contact region were calculated using the PDBsum server (Laskowski, 2009)

Figure S6. Related to Figure 6, *In vivo* autophosphorylation of WT or oncogenic KIT mutants.

Tyrosine kinase activity was compared for wild type or oncogenic KIT mutants (left panel) to those harboring an additional mutation of an Arg 381 (right panel) - residue responsible for D4:D4 homotypic contacts. WT – wild type KIT receptor; D419A – substitution of Asp 419 to Ala; ΔY418D419 – deletion of Tyr 418 and Asp 419; T417I ΔY418D419 – substitution of Thr 417 to Ile and deletion of Tyr 418 and Asp 419; Dup A502,Y503 – duplication of Ala 502 and Tyr 503; N505I – substitution of Asn 505 to Ile; V530I – substitution of Val 530 to Ile; Δ559,560 – deletion of Val 559 and 560. NIH-3T3 cells stably expressing WT or oncogenic KIT mutants were stimulated with increasing concentration of SCF (as indicated in the upper panel) for 6 minutes at 37C. Lysates of

unstimulated or SCF-stimulated cells were subject for immunoprecipitation (IP) using anti-KIT antibodies followed by SDS-PAGE and immunoblotting (IB) with anti-pTyr (IB: pTyr) or anti-KIT (IB: KIT) antibodies (as indicated).

Figure S7. Related to Figure 3, Differences in D5 dimer assembly and distances within WT KIT:SCF complex and the oncogenic T417I,ΔY418D419 mutant.
Cartoon representation of crystal structures of D5 dimers from WT KIT:SCF complex (A) and from T417I,ΔY418D419 mutant structure (B). One protomer is colored in cyan and the second in green. The center of mass of each D5 is represented by red ball. A vector depicting the orientation of each D5 is represented by red and green arrow. The distance between the center of mass of individual D5 of WT D5:D5 dimer is 24.8 Å and of the T417I,ΔY418D419 dimer structure is 16.5 Å revealing the more compact structure of the oncogenic mutant dimer. Moreover, while the D5 of KIT:SCF complex are almost parallel to each other, the D5 of the oncogenic mutant are tilted relative to each other; the angle between D5 protomers of WT and oncogenic D5 mutant are 24 and 64 degrees, respectively. Although mutant D5 dimer represents more compact structure than the WT, the distance between residues in the C-terminus is larger for mutant dimer; the distances between alpha carbons of Asn505 are 10.4 Å and 15 Å for WT and D5 mutant dimers, respectively. The more compact assembly of the mutant dimer can be also seen by comparison of the distances between A and G β strands, the major dimer interface in T417I,ΔY418D419 mutant structure. The distances between alpha carbons of Arg420 and Asn505 (the residues located in tip of A and G β strands respectively) are 14.3 Å and 4.8 Å for D5 of WT or the oncogenic D5 mutant, respectively.

Supplemental Experimental Procedures

Soluble D4D5 fragments of WT or oncogenic KIT mutants were expressed in Sf9 insect cells according to the Bac-to-Bac instruction manual (Invitrogen), using Grace's insect medium supplemented with 10% of heat inactivated fetal bovine serum. After 72 hours from the infection the cells were harvested by centrifugation at 500 g and lysed by sonication on ice in lysis buffer (100 mM potassium phosphate buffer pH 8.0 , 300 mM NaCl, 25 mM imidazole, 10% glycerol and 1% NDP-40). Crude lysate was cleared by

centrifugation at 120 000 g and filtration through 0.65 mm PVDF filter, and was applied to Ni-NTA agarose (Qiagen). Ni-NTA beads were washed with 50 column volume (CV) of wash buffer (100 mM potassium phosphate buffer pH 8.0 , 300 mM NaCl, 25 mM imidazole, 10% glycerol) and eluted with elution buffer (100 mM potassium phosphate buffer pH 8.0 , 300 mM NaCl, 250 mM imidazole, 10% glycerol). Eluted proteins were injected onto Hiload 26/600 Superdex 200 equilibrated with 10 mM Tris pH8.0, 200 mM NaCl. Fractions corresponding to KIT D4D5 fragments were combined and concentrated using Vivaspin concentrator (GE lifescience) with MWCO 10 kDa.

Purification of T417I, Δ418,419 D4D5 for structural analysis

For crystallization T417I, Δ418,419 variant of KIT D4D5 was deglycosylated with recombinant endoglycosidase F1 at final 1:50 w/w ratio, during 12 hours at room temperature. Simultaneously 6His tag was cleaved by adding 1:100 w/w ratio of recombinant TEV protease. After deglycosylation and TEV cleavage the T417I, Δ418,419 KIT D4D5 mutant was purified by anion exchange chromatography at 5/50 MonoQ column using 40 CV gradient from Buffer A (10 mM BIS-Tris pH6.5) to 50% of Buffer B (10 mM BIS-Tris pH6.5, 1M NaCl). Fractions containing the D4D5 mutant were combined, concentrated and applied to Superdex75 10/30GL, equilibrated with 10 mM TrisHCl pH 8.0, 200 mM NaCl. After size exclusion chromatography T417/I418,419 KIT D4D5 was concentrated up to 6 mg/ml and flash frozen in liquid nitrogen. For a short time protein solution was stored at 4^{o}C.

Size Exclusion and Multiangle Laser Light Scattering

Multi-Angle Light Scattering (MALS) data were collected using a Superdex 200 10/30 HR column (GE Healthcare) connected to an *Alliance* 2965 HPLC system. Elution was monitored by a photodiode array UV/VIS detector (2996 PDA, Waters Corp.), differential refractometer (RI) (OptiLab-rEx Wyatt Corp.), and static, multiangle laser light scattering detector (DAWN-EOS, Wyatt Corp.). The system was equilibrated with 20 mM HEPES, 150 mM NaCl, pH 7.5 buffer. All measurements were performed at room temperature at 0.75 ml/min flow-rate. To exclude slow equilibrium dimer formation, 0.5 ml/min flow-rate was used for each KIT D4D5 variant. Concentrations of

eluted proteins were determined using an RI detector. Weight average molecular masses were determined from Zimm plot (Wyatt, 1993). Data were analyzed using the ASTRA software package (Wyatt Technology), as described in (Folta-Stogniew and Williams, 1999).

Dissociation constants (Kd) of KIT D4D5 variants were determined by measuring the weight average molar mass across a range of protein concentrations and fitting the data by nonlinear regression to Equation 1,

$$M_w = M_r \frac{8[M]_T + K_D - \sqrt{K_D^2 + 8[M]_T K_D}}{4[M]_T} \quad \text{(Eq.1)}$$

where *M*w is the weight average molar mass (Wyatt, 1993), [*M*]*T* is the molar concentration of protein (as measured by change in refractive index), and *M*r is molecular mass of KIT D4D5 monomer. KIT D4D5 fragments were heavily glycosylated that is why average molar mass, determined by MALDI TOF was used in nonlinear regression. Nonlinear regression analysis was performed using QtiPlot open-source software.

Dup A502,Y503 D4D5 mutant

The boundaries of the Dup A502,Y503 mutant were from Val 308 to Pro 514 (numbering according to WT KIT, GNNK minus isoform). This mutant also contained a non-cleavable His tag at the C-terminus of the molecule. After thorough refinement of initial crystallization condition, large single crystals (100x80x80 μm) of the Dup D4D5 A502,Y503 mutant were obtained, but unfortunately their diffraction was not of sufficient quality for structural analysis. In order to improve diffraction quality of the Dup A502,Y503 mutant crystals, the protein sample was subjected to reductive methylation (Walter et al., 2006) followed by screening for new crystallization conditions. Methylated protein crystals were grown under similar PEG based conditions producing crystals with monoclinic $P2_1$ space group. A complete data set diffracting to 3.3 Å resolution was collected from one of the crystals of methylated Dup A502,Y503 KIT D4D5 mutant. The structure was solved by molecular replacement using D4 from the structure of ectodomain of KIT (PDB ID: 2EC8, Yuzawa et al., 2007) as a search model. Two molecules of D4 domain were found in the asymmetric unit with predicted

solvent content of 61%. Unfortunately, attempts to place D5 in this model using different D5 KIT structures as a search models (PDB ID: 2EC8, 2E9W, Yuzawa et al., 2007; 4K94 and 4K9E, Reshetnyak et al., 2013) were unsuccessful and the quality of electron density map corresponding to D5 after refinement of D4 domain structure, was not of sufficient quality for building D5 structure manually.

In order to alter crystal packing and to improve diffraction quality, an alternative construct of Dup A502,Y503 mutant containing a His tag at the N-terminus of the molecule followed by TEV cleavage site was expressed in insect cells. Moreover, constructs of different boundaries (V308-P514 or V308-A507) were expressed and methylated or non-methylated proteins were screened for initial crystallization conditions. Diffraction quality crystals of methylated Dup A502,Y503 mutant KIT D4D5 $_{V308\text{-}A507}$ (Fig 1C) were grown and a complete data set of 2.9 Å resolution was collected. This protein form also crystallized in monoclinic $P2_1$ space group, with 6 molecules per asymmetric unit. Single solution was found using KIT D4 domain as a search model, but attempts to place D5 domain by molecular replacement or build it manually were unsuccessful. Clearly, the structural analysis showed that the Dup A502,Y503 formed dimers in which the D4:D4 interface seen in the crystal structure of the SCF stimulated dimers of KIT ectodomain was maintained (Figure S5 and Yuzawa et al., 2007). However, the exact structure of the D5:D5 interface of the Dup A502Y503 oncogenic mutant could not be determined.

Dup A502,Y503 D4D5 mutant crystallization procedures

Dup502,503 $D4D5_{308\text{-}514}$ with His tag at the C-terminus and Dup502,503 $D4D5_{308\text{-}507}$ were both subject for reductive methylation using Jena Bioscience JBS methylation kit (cat. number CS-510) according to instruction manual. Dup502,503 $D4D5_{308\text{-}514}$ was crystallized at 22^{o}C from 16% PEG 10000, 0.1 M HEPES pH 7.4, crystals were cryoprotected with reservoir solution supplemented with 25% glycerol and flash frozen in a liquid nitrogen. Dup502,503 $D4D5_{308\text{-}507}$ crystallized from 20% PEG 10000, 0.1 M Tris pH 8.2, crystals were transferred into cryoprotectant solution (25% PEG 10000, 0.1 M Tris pH 8.2 and 2M sodium formate), mounted into cryoloops and flash frozen. X-ray

diffraction data were collected at X25 beamline at the National Synchrotron Light Source (NSLS). All data were processed and scaled using HKL2000 program package (Otwinowski and Minor, 1997).

REFERENCES

Folta-Stogniew, E., and Williams, K.R. (1999). Determination of molecular masses of proteins in solution: Implementation of an HPLC size exclusion chromatography and laser light scattering service in a core laboratory. J. Biomol. Tech. *10*, 51–63.

Laskowski, R.A. (2009). PDBsum new things. Nucleic Acids Res. 37, D355–9.

Otwinowski, Z., and Minor, W. (1997). Processing of X-ray diffraction data collected in oscillation mode. Methods Enzymol. 276, 307–326.

Reshetnyak, A. V, Nelson, B., Shi, X., Boggon, T.J., Pavlenco, A., Mandel-Bausch, E.M., Tome, F., Suzuki, Y., Sidhu, S.S., Lax, I., et al. (2013). Structural basis for KIT receptor tyrosine kinase inhibition by antibodies targeting the D4 membrane-proximal region. Proc. Natl. Acad. Sci. U. S. A. 110, 17832–17837.

Yuzawa, S., Opatowsky, Y., Zhang, Z., Mandiyan, V., Lax, I., and Schlessinger, J. (2007). Structural basis for activation of the receptor tyrosine kinase KIT by stem cell factor. Cell 130, 323–334.

Walter, T.S., Meier, C., Assenberg, R., Au, K.-F., Ren, J., Verma, A., Nettleship, J.E., Owens, R.J., Stuart, D.I., and Grimes, J.M. (2006). Lysine methylation as a routine rescue strategy for protein crystallization. Structure 14, 1617–1622.

Wyatt, P. (1993). Light scattering and the absolute characterization of macromolecules. Anal. Chim. Acta *272*.